JPMTR 132 | 1910
DOI 10.14622/JPMTR-1910
UDC 676.2:538.3|53.07

Original scientific paper
Received: 2019-10-28
Accepted: 2020-05-28

An empirical model for describing the mechanical behavior of paper and paper stacks in the perpendicular to the in-plane direction

Jian Chen[1], *Dieter Spiehl*[2], *Edgar Dörsam*[2], *Arash Hakimi Tehrani*[2] *and Simon Weißenseel*[2]

[1] School of Mechanical Engineering, Yangzhou University, Huayang Weststr. 196, 225127 Yangzhou, China — chenjian.tud@hotmail.com
[2] Institute of Printing Science and Technology, Technische Universität Darmstadt, Magdalenenstr. 2, 64289 Darmstadt, Germany — spiehl@idd.tu-darmstadt.de, doersam@idd.tu-darmstadt.de, arash.hakimi.t@gmail.com, simon.weissenseel@alcon.com

Abstract

The mechanical behavior of paper materials under compression in the out-of-plane direction is highly nonlinear. If the influence of the surface topography is not taken into account, the stress–strain curve of paper materials in the loading process is a typical example of materials with J-shaped compressive curves. When compression is released, the stress–strain curve in the unloading process is also nonlinear. The main purpose of this paper is to establish a suitable mathematical model and actualize the description of the compression curve for paper and paper stacks. The loading and unloading nonlinearities of paper stress–strain relations can be approximated by using different equations. In this paper, the loading curve of paper is calculated by using the sextic polynomial equation and the unloading curve is described by using the modified exponential function. All the used coefficients for determining the functions are expressed as the functions of the stress at the start point of unloading. The compressive behavior of paper under some given forces are also calculated by using the identified equation and verified by means of the experimental data. For multiple sheets, it is assumed that when the force is the same, the deformation of the paper stack is directly proportional to the number of sheets. Based on this assumption, the force–deformation relation of the paper stack is derived. The comparative analysis of the experimental results demonstrates the effectiveness of the description model.

Keywords: out-of-plane direction, loading and unloading stages, stress–strain relationship, force–deformation curve, paper and paper stacks

1. Introduction and background

The mechanical stress–strain curve of paper is obviously affected by many factors, such as: the surface roughness, temperature, humidity as well as compression speed, etc. The properties of paper have been studied in numerous papers. But until now, it is still very hard to build a unified model which can be perfectly used for paper or paper stack and consider all of these factors. According to different classification criteria, the paper models can be classified into various groups.

Depending on whether the surface topography is taken into account, the analysis models of paper can be divided into rough surface models and smooth solid models. Generally, the paper is modelled as smooth solid material; the ignorance of the surface roughness brings lots of convenience for analyzing the processes such as paper delivery and paper calendering (Eckstein, 2014, p. 140). An analytical model was developed by Litvinov and Farnood (2010) for the compression of coated substrates in a soft rolling nip, in which, the substrate was represented by a modified solid element. The surface topographical differences between the cross direction and the machine direction for newspaper and paperboard were investigated by Alam, et al. (2011). When compressing thin sheets, it is very important to be aware of the influence of surface roughness (Rättö, 2005). The surface topography plays an important role in obtaining the stress–strain curve of paper materials; different methods of calculating the

contact area will lead to very different results (Chen, et al., 2016a). The influence of surface roughness was also discussed in some papers, for example, the paper surface topography under compression was studied by Teleman, et al. (2004). According to the surface topography, the paper body was considered as being composed of two rough surfaces and an internal structure (Schaffrath and Göttsching, 1991; Chen, Neumann and Dörsam, 2014), the force–deformation relationship of paper was derived by using the Newton formula.

Based on the law of the essential physical characteristic of materials, the models of paper materials can be divided into constitutive models (Ramasubramanian and Wang, 1999; Xia, Boyce and Parks, 2002; Stenberg, 2003) and non-constitutive models. For the constitutive models, the properties of paper such as elasticity, plasticity and viscosity were modelled by using spring, dry friction and dashpot elements, respectively (Agilar Ribeiro and Costa, 2007; Gavelin, 1949). According to those methods, the differences of these constitutive models mainly lie in the different combinations of these elements. A considerable number of free parameters have to be determined by doing experiments in these constitutive models. Moreover, most of these parameters are very difficult to be measured.

In addition, according to different research methods, the research of paper can also be classified as experimental, simulation or mathematical analysis, etc. Four different experimental methods were evaluated for characterizing the smoothness of the handsheets (Singh, 2008; Nygårds, et al., 2005; Pino and Pladellorens, 2009). Some references (Mäkelä and Östlund, 2003; Ramasubramanian and Wang, 2007; Nygårds, et al., 2005; Andersson, 2006, p. 73; Lavrykov, et al., 2012) attempted to establish the simulation model for paper and paperboard in finite element method (FEM) software. Creasing and folding of multiply paperboard were also simulated by Huang with co-workers (Huang and Nygårds, 2010; 2012; Huang, Hagman and Nygårds 2014). Hill (1950) established Hill material with isotropic hardening. An anisotropic in-plane and out-of-plane elasto-plasto continuum model for paperboard consistent with the laws of thermodynamics was built by Borgqvist with co-workers, the creasing (Borgqvist, et al., 2015) and folding (Borgqvist, et al., 2016) operations were studied and compared to experimental results. In addition, an elastic-plastic model and the cohesive zone model (CZM) was proposed by Li, Reese and Simon (2017) to simulate the paperboard creasing process. Chen et al. (2015) proposed that the simulation of paper in the perpendicular to the in-plane direction can be solved by using the gasket model and avoiding the difficult measurements required for obtaining the parameters in previous models.

Compared to the in-plane dimensions, the thickness of paper material is very thin. It may sometimes be hard to imagine the use for an out-of-plane material model (Stenberg, 2002, p. 18). However, the mechanical behavior of paper has a very close relationship with many operations in the papermaking or printing industries, such as paper calendering, folding, creasing, traditional printing, and so on. The research on multiple sheets is also closely related to many applications, such as the operations of moving and organizing of paper in the pre-printing stage, paper cutting, book binding and paper counting in the post-printing process, and so on. Most of these examples have been described in Stenberg (2002, p. 18) in detail. In these examples, the importance of the out-of-plane behavior is enhanced.

For multiple sheets, a characteristic equation for paper pile in exponential form was proposed by Pfeiffer (1981) and the *K1* and *K2* factors were measured for paper stacks. When the surface roughness of paper was taken into consideration (Schaffrath and Göttsching, 1991), the force–deformation behavior of paper stack was investigated. Based on the model proposed by Schaffrath and Göttsching (1991), a theoretical formula was built for paper pile (Arango Diaz, Pfirrmann and Schmitt, 2009) to show the relationship between height and number of sheets; the force–deformation behavior of multiple sheets was also investigated (Chen, et al., 2016b). However, the simulation work and the research about paper stacks are still not sufficient, and therefore should be one of the main research directions in the future.

According to the knowledge of the authors, the compressive curve of paper material is a typical example of materials with J-shaped stress–strain curves, which is very similar to gasket and biomaterials (DoITPoMS, 2004). The curve shows that initially, small increases in stress give large deformations, however, at larger deformations the material becomes stiffer and more difficult to be compressed. A mathematical description model for spiral wound gasket was proposed by Takaki and Fukuoka (2000), then the stress–strain relation for asbestos sheet gasket was proposed by Takaki and Fukuoka (2001) in the same way. After that, these models were widely used for calculating the stress–strain curve of gasket materials (Takaki and Fukuoka, 2002a, 2002b, 2003; Nagata, Shoji and Sawa, 2002; Fukuoka and Takaki, 2003; Fukuoka, et. al., 2007; Fukuoka, Nomura and Nishikawa, 2012), especially, for the FEM calculation of gasket materials. The same method was used in this paper for establishing the empirical model for paper materials.

The aim of this study is to establish the empirical model and actualize the description of the stress–strain curve of paper sheet under the out-of-plane compression.

By establishing the empirical model, the stress–strain behavior of paper under different compressive forces in the through-thickness direction will be deeply investigated. Based on the stress–strain relation, the model for describing the force–deformation curve of paper stacks will also be derived. Finally, a comparison of the modelling results will be carried out with the experimental data.

2. Materials and methods

2.1 Theoretical basis

The stress–strain curve of paper consists of two parts: the curve under loading condition and the curve under unloading condition. Because of the plasticity of the paper material, the analysis of the unloading curve is much more complicated than the loading curve, but anyway, both can be described by using curve fitting methods. Generally, the description models for J-shaped materials can be divided into linear and nonlinear models.

For the compression behavior of gasket material, Nagata, Shoji and Sawa (2002) proposed a simplified linear model, in which the nonlinearity of the gasket stress–strain relation was approximated by two elastic moduli in loading and unloading stages, respectively. The comparison of computing results between the simplified linear model and the nonlinear model was also provided. For the analysis of gasket stress distribution in bolted flange joints, the result of this simplified model gives a good agreement with the result of nonlinear model.

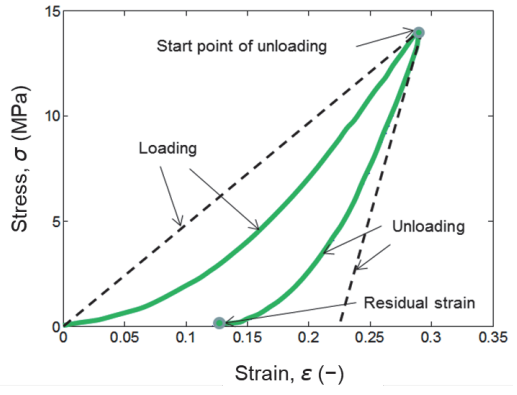

Figure 1: Typical stress–strain curve of paper shown in green color; the black dotted line is the simplified linear stress–strain curve of paper modelled with two elastic springs

The material behavior of paper in the out-of-plane direction (*z*-direction, ZD) can also be modelled with two linear springs (as shown in Figure 1), which provides convenient analysis of processes such as paper delivery and paper calendering (Eckstein, 2014, p. 140). As mentioned previously, a characteristic equation for paper pile in exponential form was proposed by Pfeiffer (1981), both of the stress–strain curves in loading and unloading stages were expressed by using exponential functions with coefficients of *K1* and *K2*.

In this paper, a polynomial function and a modified exponential function are used respectively for describing the stress–strain curve of paper on the loading condition and the unloading condition.

2.2 Numerical analysis

According to the model proposed by Takaki and Fukuoka (2000), the stress–strain curve of spiral wound gasket in the loading process can be described by using the sextic polynomial function:

$$\sigma = a_0 + a_1 \cdot \varepsilon + a_2 \cdot \varepsilon^2 + a_3 \cdot \varepsilon^3 + a_4 \cdot \varepsilon^4 + a_5 \cdot \varepsilon^5 + a_6 \cdot \varepsilon^6 \quad \text{[MPa]} \qquad [1]$$

where σ and ε are the paper stress and strain, respectively. The a_i (i = 0, ..., 6) are constant values for identifying the polynomial function. Generally, a_0 = 0, but before the loading process, a preload is put on the specimen, so the corresponding value of a_0 is not 0.

For the unloading curve, the stress–strain relationship can be described by using the modified exponential function; the idea of constructing the model is to ensure that the established equation goes through the residual strain point (ε_r, 0):

$$\sigma = \alpha \cdot \exp(\beta \cdot \varepsilon) - \alpha \cdot \exp(\beta \cdot \varepsilon_r) \quad \text{[MPa]} \qquad [2]$$

where:

$$\beta = f_1(\varepsilon_{spu}) = a + b \cdot \varepsilon_{spu} + c \cdot (\varepsilon_{spu})^{\frac{1}{3}}$$
$$\varepsilon_r = f_2(\varepsilon_{spu}) = p \cdot \varepsilon_{spu} + q \qquad [3]$$
$$\alpha = f_3(\varepsilon_{spu}) = \frac{\sigma_{spu}}{\exp(\beta \cdot \varepsilon_{spu}) - \exp(\beta \cdot \varepsilon_r)}$$

In Equations [2] and [3], σ is the dependent variable and ε is the independent variable. The unloading curve is determined by the coefficients α and β. The σ_{spu} and ε_{spu} are the values of stress and strain at the start point of unloading, respectively. The value of σ_{spu} can be calculated according to Equation [1]. The a, b and c are the constants for identifying the relationship between β and ε_{spu}. The p and q are the components of the equation between ε_r and ε_{spu}. All of the coefficients α, β and ε_r can be expressed as a function of the independent variable ε_{spu}.

Furthermore, the relationship between force and deformation can be converted from the stress–strain relation by using the following equations:

$$F = \sigma \cdot \pi \cdot \left(\frac{d_{\text{dia}}}{2}\right)^2 \quad [\text{N}] \qquad [4]$$
$$z = \varepsilon \cdot d_{\text{thi}} \quad [\text{mm}]$$

where, F is the force imposed on the paper specimen and z is the deformation of paper under the corresponding force F. The diameter of the cylindrical indenter is d_{dia}. The average thickness of paper is d_{thi}. According to Equations [1] to [4], the force–deformation relation of one sheet can be divided into two parts and expressed as:

$$F_{1,\,\text{loading}} = \left\{\sum_{i=0}^{6}\left[a_i \cdot \left(\frac{z_{1,\,\text{loading}}}{d_{\text{thi}}}\right)^i\right]\right\} \cdot \pi \cdot \left(\frac{d_{\text{dia}}}{2}\right)^2 \quad [\text{N}] \qquad [5]$$

$$F_{1,\,\text{unloading}} = \left\{\alpha \cdot \exp\left[\beta \cdot \left(\frac{z_{1,\,\text{unloading}}}{d_{\text{thi}}}\right)\right] - \alpha \cdot \exp(\beta \cdot \varepsilon_{\text{r}})\right\} \cdot \pi \cdot \left(\frac{d_{\text{dia}}}{2}\right)^2 \quad [\text{N}]$$

in which, $F_{1,\,\text{loading}}$ and $F_{1,\,\text{unloading}}$ are the forces in the loading stage and unloading stage, respectively, $z_{1,\,\text{loading}}$ and $z_{1,\,\text{unloading}}$ are the corresponding deformations, the subscript 1 corresponds to 1 sheet.

For multiple sheets, it is assumed that when the force is the same, the deformations of the paper stack $z_{n,\,\text{loading}}$ and $z_{n,\,\text{unloading}}$ are directly proportional to the number of sheets n. On the basis of this assumption, the force–deformation relation can be expressed as:

$$z^n_{\text{loading}} = k_{\text{loading}} \cdot n \quad [\text{mm}] \qquad [6]$$

$$z^1_{\text{unloading}} = k_{\text{unloading}} \cdot n \quad [\text{mm}]$$

In Equation [6], k_{loading} and $k_{\text{unloading}}$ are the slopes in the loading and unloading conditions, respectively, which are used for showing the relationship between deformation and number of paper sheets.

The values of k_{loading} and $k_{\text{unloading}}$ depend on the independent variable forces; when force changes, the values of k_{loading} and $k_{\text{unloading}}$ also change. The relationship between the slope and force can be expressed as the following equations:

$$k_{\text{loading}} = f_4\left(F^1_{\text{loading}}\right) \qquad [7]$$

$$k_{\text{unloading}} = f_5\left(F^1_{\text{unloading}}\right)$$

According to Equations [6] and [7], the force–deformation relation model of one sheet derived in Equation [5] can be extended to multiple sheets:

$$z_{n,\,\text{loading}} = f_4\left(F_{1,\,\text{loading}}\right) \cdot n \quad [\text{mm}] \qquad [8]$$
$$F_{n,\,\text{loading}} = F_{1,\,\text{loading}} \quad [\text{N}]$$
$$z_{n,\,\text{unloading}} = f_5\left(F_{1,\,\text{loading}}\right) \cdot n \quad [\text{mm}]$$
$$F_{n,\,\text{unloading}} = F_{1,\,\text{unloading}} \quad [\text{N}]$$

where $F_{n,\,\text{loading}}$ and $F_{n,\,\text{unloading}}$ are the forces applied to paper stack in the loading and unloading condition, respectively. For a better understanding, the force–deformation relation of multiple sheets can also be expressed as the converse equation of Equation [8]:

$$F_{\text{n,\,loading}} = f_4^{-1}\left(\frac{z_{\text{n,\,loading}}}{n}\right) \quad [\text{N}] \qquad [9]$$

$$F_{\text{n,\,unloading}} = f_5^{-1}\left(\frac{z_{\text{n,\,unloading}}}{n}\right) \quad [\text{N}]$$

2.3 Material and experimental setup

The paper used here for verifying the proposed model is the copy paper (Copy paper, DIN A4, 210 × 297 mm, 80 g/m^2), produced by the Steinbeis Paper GmbH in the year 2013. The actual average thickness is d = 84.7 µm.

The measurements were performed on the universal testing machine Zwick Z050, which can be utilized for strain, shear and bending tests with different substrates and machine components with high accuracy of the cross head speed (0.0005–2 000 mm/min), and position repetition accuracy (± 2 µm). The compression equipment is shown in Figure 2, which was designed by Kaulitz (2009, p. 179).

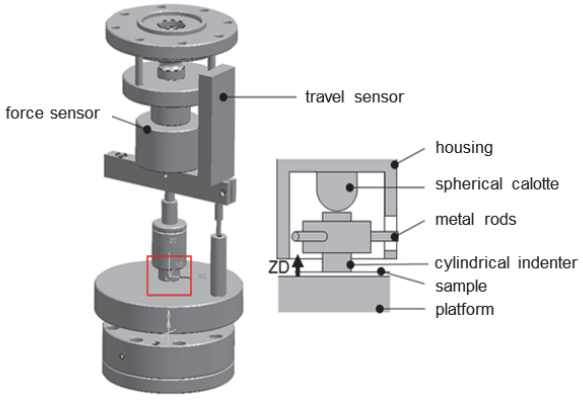

Figure 2: Test equipment for obtaining the force–deformation curve of the paper constructed by Kaulitz (Kaulitz, 2009, p. 179); the diameter of the cylindrical indenter (pressure head) is 6 mm

To eliminate the effect of climate conditions of the environment on the mechanical force–deformation behavior, the experimental studies were performed under standardized climatic conditions. The climate is specified in DIN 50014 and prescribed a range of 23 ± 0.5 °C for the temperature and a range of 50 ± 1.5 % for the relative humidity (Deutsche Institut für Normung, 2018).

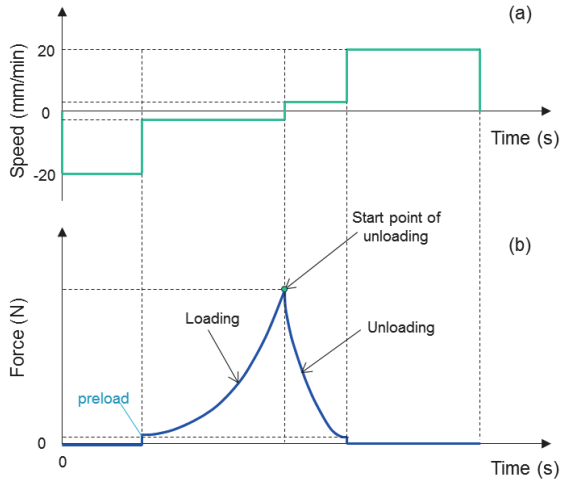

Figure 3: Schematic of the applied speed and force in loading cycle; (a) shows the changes of speed in a complete cycle, negative value means the speed is opposite to ZD direction, see Figure 2, (b) shows the corresponding forces; the strain rate is about 0.01

Figure 3 shows the settings of the loading speed and the corresponding force. At the beginning of the loading condition, the cylindrical indenter moves down from the original position at the speed of 20 mm/min, until the indenter comes into contact with the surface of the paper. The preload here is set to 1 N; when the change of force is 1 N, the compression process will begin with a velocity of 0.05 mm/min. After the force reaches the desired maximum force, the indenter will move up at the speed of 0.05 mm/min. When the force decreases to 1 N, the indenter returns back to the original position at the speed of 20 mm/min. The average thickness of paper is d = 84.7 µm, so, both in the loading and unloading process, the strain rate is equal to the loading speed divided by the thickness of paper; the value is about 0.01.

According to the size of the indenter (the diameter of the indenter is 6 mm) and paper thickness, the force–deformation curve can be easily transferred into the stress–strain curve by using Equation [4].

The obtained data of experiments can also be used for establishing the descriptive model for paper materials and comparing its results with the calculation results under different forces.

3. Results

3.1 Summary of the model for one sheet

For the loading process of one sheet, the stress–strain curve can be described by using the curve fitting method, by which, a set of experimental force–deformation data were needed. With the aid of suitable software, such as Matlab (Matlab Help, 2013), the constants which are used for identifying the loading curve of paper can be calculated automatically according to Equation [1]. All values of a_i coefficients are shown in Figure 4.

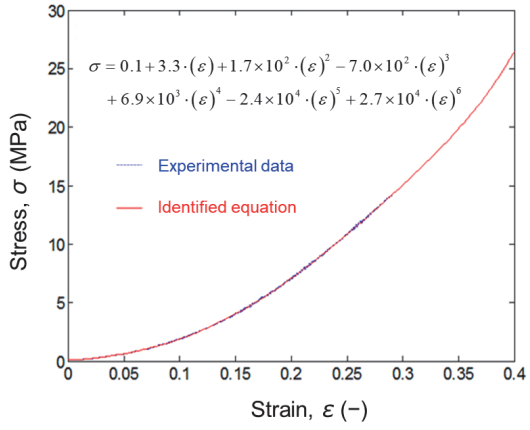

Figure 4: Stress–strain curve of paper in the loading condition; the blue curve is the experimental curve, the red one is the fitting curve by using the polynomial function; the coefficient of determination: R^2 = 1.0

From Figure 4, it can be seen that the stress–strain curve of paper in the loading stage can be described by using the polynomial function. The stress–strain curve under any desired strain can be obtained by the following identified equation.

$$\sigma = 0.1 + 3.3\cdot\varepsilon + 1.7\times10^{2}\cdot\varepsilon^{2} - 7.0\times10^{2}\cdot\varepsilon^{3} + 6.9\times10^{3}\cdot\varepsilon^{4} - 2.4\times10^{4}\cdot\varepsilon^{5} + 2.7\times10^{4}\cdot\varepsilon^{6} \quad [\text{MPa}] \qquad [10]$$

For the unloading process, the model is built according to Equations [2] and [3]. There are three unknown variables, α, β and ε_r; the different values of ε_r under different forces can be directly obtained from the experimental data. Two more groups of point coordinates, (ε_{spu}, σ_{spu}) and (ε_m, σ_m), are selected for calculating the coefficients α and β. As shown in Figure 5, ε_{spu} and σ_{spu} are the strain and stress values at the start point of unloading. The point (ε_r, 0) represents the residual strain. The (ε_m, σ_m) is a random point selected in the unloading curve. With the help of these points, the values of α and β can be easily calculated.

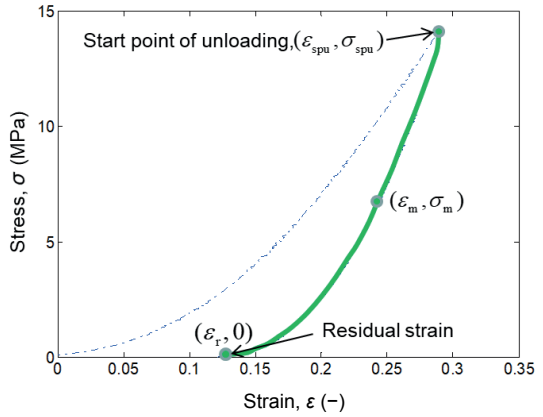

Figure 5: Selected points in the unloading stress–strain curve for calculating the components identifying the unloading function

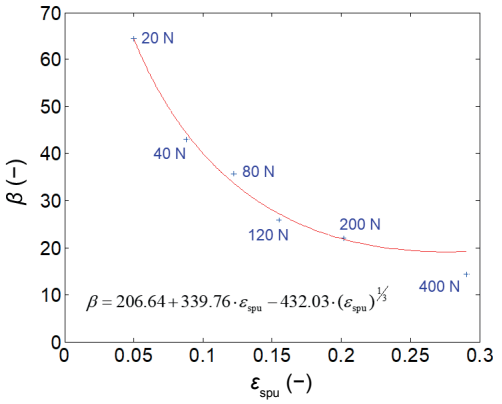

Figure 6: Relationship between the coefficients β and ε_{spu}; the discrete points are the points listed in Table 1, the red curve is calculated by using the curve fitting method

3.2 Relationship between coefficient β and strain ε_{spu}

As mentioned above, three groups of point coordinates are needed for calculating the values of α and β. For instance, when the maximum force applied on the paper is 80 N, the value of ε_r can be obtained from the experiment. Then combined with the values at the start point of unloading (ε_{spu}, σ_{spu}) and the random point (ε_m, σ_m), the value of β can be calculated. The final calculation result of β under 80 N is 35.73. Other values of β can be calculated in the same way and the results are listed in Table 1.

Table 1: Values of ε_{spu} and β under different forces

Force (N)	ε_{spu} (–)	β (–)
20	0.0502	64.52
40	0.0880	43.03
80	0.1222	35.73
120	0.1547	25.97
200	0.2019	22.04
400	0.2904	14.36

According to the data obtained in Table 1, it can be observed that the values of β are decreasing with the increasing of ε_{spu} values; these discrete points have been plotted in the following coordinates in Figure 6.

As shown in Figure 6, the coefficient β is regarded as a dependent variable, which changes with the independent variable ε_y; the relation between them can be expressed by the following function:

$$\beta = f_1(\varepsilon_{spu}) = 206.64 + 339.76 \cdot \varepsilon_{spu} - 432.03 \cdot (\varepsilon_{spu})^{1/3} \quad [11]$$

The function above consists of two parts: a linear polynomial function and a radical function. Here, the coefficients provided in Equation [3] are: a = 206.64, b = 339.76 and c = 432.03. The coefficient of determination is R^2 = 0.994. This function can also be expressed by using other functions, for example, the exponential function. The comparison between them will be implemented in the discussion chapter.

3.3 Relationship between strains ε_r and ε_{spu}

As mentioned previously, (ε_{spu}, σ_{spu}) represents the start point of unloading and (ε_r, 0) is the residual strain point. The values of ε_{spu} and ε_r can be directly obtained from the experimental data. The values under different forces are listed in Table 2.

Table 2: Values of ε_{spu} and ε_r under different forces, which have been obtained according to the experimental results

Force (N)	ε_{spu} (–)	ε_r (–)
20	0.0502	0.0024
40	0.0880	0.0159
80	0.1222	0.0272
120	0.1547	0.0460
200	0.2019	0.0756
400	0.2904	0.1216

On the basis of the data listed in Table 2, it can be seen that the values of ε_r are increasing with the increasing of ε_{spu} values; these discrete points were plotted in Figure 7. The values of ε_{spu} and ε_r are regarded as abscissa and ordinate, respectively.

From Figure 7, it can be seen that the relationship between ε_r and ε_{spu} is linear. By using the linear curve fitting method, the relationship between residual

strain ε_r and the corresponding unloading strain ε_{spu} can be expressed as:

$$\varepsilon_r = f_2(\varepsilon_{spu}) = 0.49 \cdot \varepsilon_{spu} - 0.027 \quad [12]$$

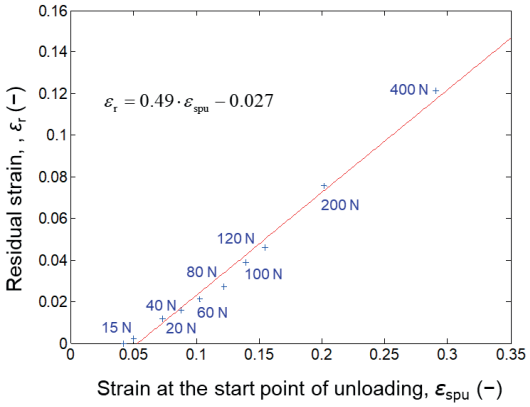

Figure 7: Relationship between the maximum strain and the residual strain; the red curve is calculated by using the linear curve fitting method

The coefficients of linear relation proposed in Equation [3] are: p = 0.49, q = −0.027. The coefficient of determination is R^2 = 0.990.

3.4 Relationship between coefficient α and strain ε_{spu}

According to Equation [3], the value of α is determined by the values of β and ε_r; the value of β can be calculated by using Equation [11], the value of ε_r is expressed as Equation [12]. The final function of α can be expressed as follows:

$$\alpha = f_3(\varepsilon_{spu}) = \frac{\varepsilon_{spu}}{\exp(\beta \cdot \varepsilon_{spu}) - \exp(\beta \cdot \varepsilon_r)} \quad [13]$$

3.5 Relationship between $k_{loading}$ and $F_{loading}$

For multiple sheets, the description model was constructed on the assumption that when the force is the same, the deformation of paper stack ($z_{n,\,loading}$ and $z_{n,\,unloading}$) is proportional to the number of sheets n. This hypothesis was verified by the experimental data.

It can be seen from Figure 8 that, when the force is 100 N, the deformation of paper stacks at the start points of unloading shows a perfectly linear relationship with the sheet numbers.

For the curve fitting function, the coefficient of determination is R^2 = 0.999. For other forces, the experimental result is shown in Figure 9; the curve indicates linear relationship between deformation and sheet number.

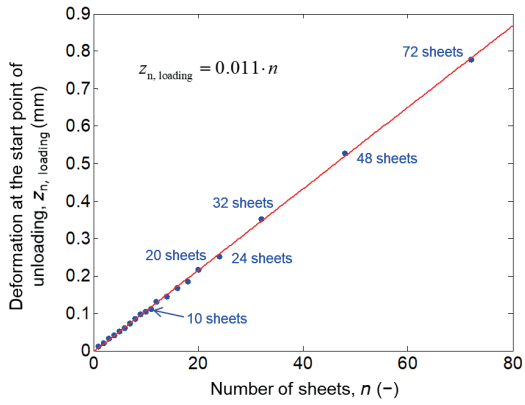

Figure 8: Deformation of different paper stacks under the same force; the force applied here is 100 N, the red curve is the linear curve fitting result

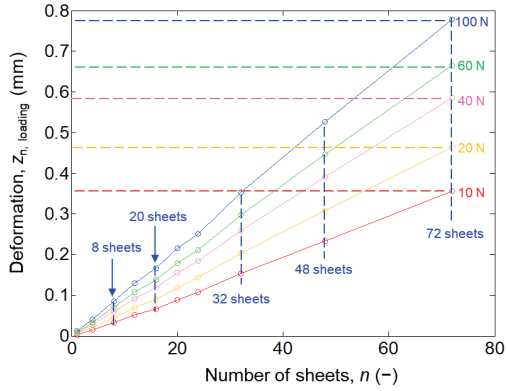

Figure 9: Experimental deformation of paper stacks under different loading forces

For different number of sheets, the statistical deformation value under different forces has been plotted in Figure 9, from which we can see the linear relationship between deformation and sheet number under different forces. The values of the slopes can be calculated and the values of forces and slopes are listed in Table 3.

Table 3: The values of $k_{loading}$ under seven groups of different loading forces

Group	$F_{loading}$ (N)	$k_{loading}$ (–)
1	5	0.0036
2	10	0.0050
3	20	0.0065
4	40	0.0082
5	60	0.0093
6	80	0.0100
7	100	0.0110

According to the listed slope values ($k_{loading}$) in Table 3, the values of slopes and forces were plotted in the same coordinate system; the value of $F_{loading}$ is regarded as the abscissa. The value of $k_{loading}$ is regarded as the ordi-

nate. Then, the values of the slopes can be expressed as the function of forces.

Figure 10 displays that the value of k_{loading} is changing with force; the relationship between them can be approximated by using different functions.

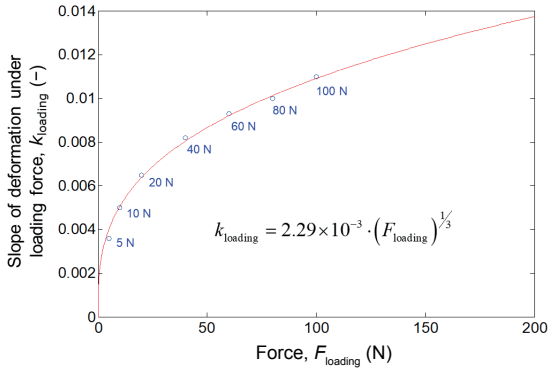

Figure 10: Relationship between the slopes and the forces in the loading condition; the discrete blue points are the values of $k_{loading}$ under different forces, the red curve is the approximation curve

A radical function was used here for describing the relationship between slope and force. The coefficient of the function can be calculated by using the curve fitting method. The coefficient of determination is $R^2 = 0.997$.

$$z_{n,\,\text{loading}} = \left[2.29\times10^{-3}\cdot\left(F_{n,\,\text{loading}}\right)^{1/3}\right]\cdot n \quad \text{[mm]} \qquad [14]$$

3.6 Relationship between $k_{\text{unloading}}$ and $F_{\text{unloading}}$

The same as in the loading stage, for different forces, the slopes in the unloading stage are also constant values, which can be seen in Figure 11. However, because of the plasticity of the paper materials, a part of the deformation of paper in the unloading process cannot be recovered to the original shape, which is a non-reversible change of shape in response to applied force.

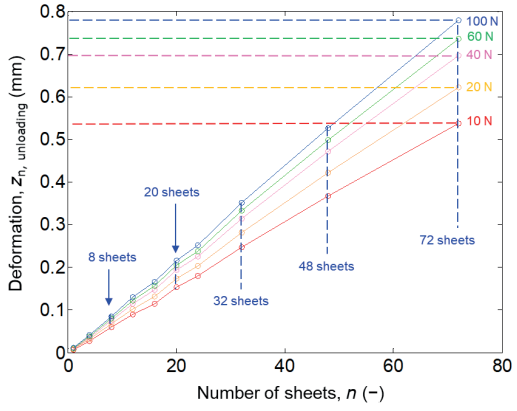

Figure 11: Experimental deformation of paper stacks under different unloading forces

The non-recoverable part shown in the force–deformation curve is called the residual deformation. The corresponding strain shown in the stress–strain curve is called the residual strain, which is shown in Figure 1 and Figure 5. Thus, in the unloading stage, when the force is decreasing to 0 N, the deformation of paper stacks cannot recover to 0 mm. But for simplifying the model, the influence from the residual deformation is ignored.

And the same, for different sheets, when the force is the same, the total deformation is directly proportional to the number of sheets; the values of the slopes under different groups of forces are shown in Table 4.

Table 4: The values of $k_{unloading}$ under seven groups of different loading forces

Group	$F_{\text{unloading}}$ (N)	$k_{\text{unloading}}$ (–)
1	5	0.0063
2	10	0.0076
3	20	0.0087
4	40	0.0098
5	60	0.0100
6	80	0.0110
7	100	0.0110

The values of slopes and forces listed in Table 4 are plotted in the same coordinate system; the values of $F_{\text{unloading}}$ and $k_{\text{unloading}}$ are regarded as the horizontal and ordinate axis, respectively. By using the curve fitting method, the values of the slopes can be expressed as the function of forces. The relation between $k_{\text{unloading}}$ and $F_{\text{unloading}}$ can be calculated according to the obtained function in Figure 12. The coefficients of the function are calculated by using the curve fitting method. Two radical functions are used for describing the relationship between slope and force. As mentioned above, the influence of the residual deformation is ignored; the values of slopes are regarded as changing from 0.

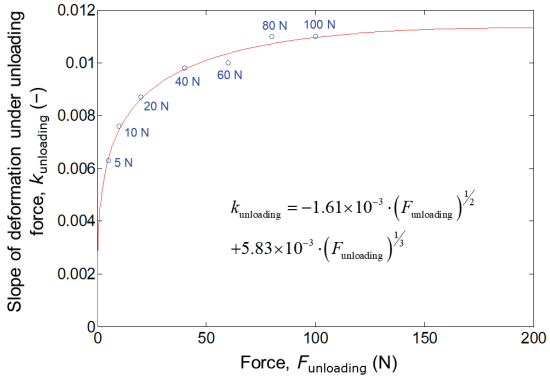

Figure 12: Relationship between the slopes and the forces in the unloading condition, the discrete blue points are the values of $k_{unloading}$ under $F_{unloading}$, the red curve is the fitting curve

The function of the unloading deformation can be expressed as:

$$z_{n,\,\text{unloading}} = \left[-1.61\times10^{-3}\cdot\left(F_{n,\,\text{unloading}}\right)^{1/2} + 5.83\times10^{-3}\cdot\left(F_{n,\,\text{unloading}}\right)^{1/3}\right]\cdot n \quad \text{[mm]} \qquad [15]$$

The coefficient of determination is $R^2 = 0.988$.

3.7 Final calculation model

The stress–strain relation of one sheet can be expressed by Equations [1] to [3] and [10] to [13]. The force–deformation relation of paper stack can be expressed by Equations [4] to [9] and [14] and [15].

3.8 Comparisons between the experimental data and the empirical results

In order to verify the applicability of the proposed model, some experiments on paper by using different maximum compression forces were performed; their results are shown in Figure 13. In the experimental process, the provided maximum forces were 20 N, 60 N, 80 N and 120 N.

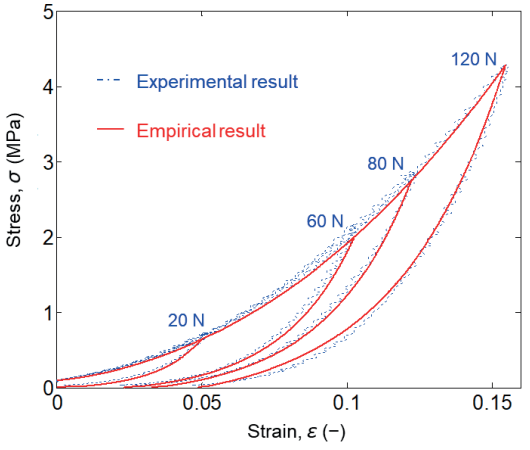

Figure 13: Comparisons between the experimental and empirical stress–strain curves of one sheet; the blue curves are the experimental results, the red curves were calculated by using the empirical model, using Equations [1] to[3] and [10] to [13]

Figure 13 shows the comparisons between the experimental and the calculated stress–strain curve of paper. The empirical and experimental results fit fairly well. The results show that this description model is capable of capturing the stress–strain behavior of paper at a wide range of strains.

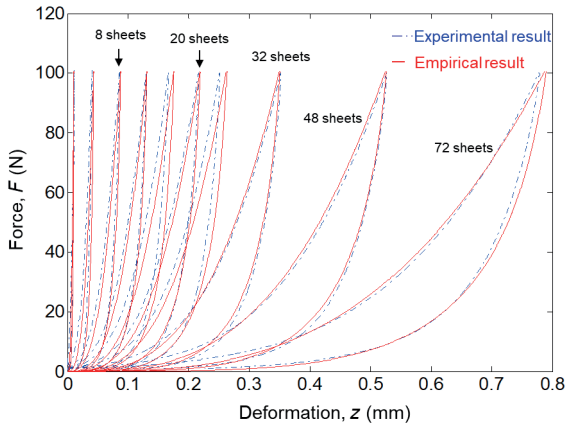

Figure 14: Comparisons between the experimental and empirical force–deformation curves of paper stacks; the blue curves are the experimental force–deformation data, the red curves were calculated by using the empirical model, Equations [4] to [9] and [14] and [15]

As shown in Figure 14, some experiments of multiple sheets (1, 4, 8, 12, 16, 20, 24, 32, 48, 72 sheets) with maximum force of 100 N were implemented. Comparison of the experimental results with empirical calculated results is shown in this figure. The deformations of paper stacks under the maximum force were selected for calculating the deviation.

The deviations for different numbers of sheets are listed in Table 5, with the largest values for 4, 16 and 24 sheets, but still within ±5 %. The model calculations give good fits to the experimental results.

Table 5: Comparisons of the force–deformation curves of paper pile between the experimental and empirical results, which is based on the deformation at the start point of unloading

Number of sheets	Deformation at the start point of unloading (mm)		Deviation (%)
	Experimental result	Empirical result	
4	0.042	0.044	−4.76
8	0.085	0.087	−2.35
12	0.130	0.131	−0.76
16	0.167	0.175	−4.79
20	0.216	0.219	−1.39
24	0.251	0.262	−4.38
32	0.352	0.350	+0.57
48	0.527	0.525	+0.38
72	0.778	0.787	−1.16

4. Discussion

4.1 Discussion about the stress–strain relation of one sheet

The loading process can be described by using not only polynomial function, but also exponential function defined in Equation [16] (Figure 15). The comparisons between them are discussed here.

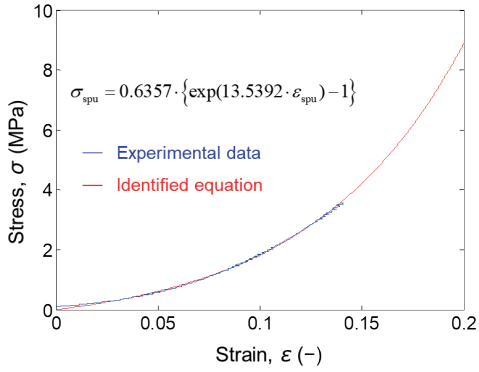

Figure 15: Stress–strain curve of paper in the loading stage; the blue curve is the experimental result, the red curve is calculated by using the exponential function

$$\sigma = p_1 \cdot [\exp(q_1 \cdot \varepsilon) - 1] \quad [\text{MPa}] \qquad [16]$$

where p_1 and q_1 are the coefficients for determining the loading exponential function, which can be calculated by using the curve fitting method; the result is shown in Equation [17]. The coefficient of determination is $R^2 = 0.998$.

$$\sigma_{\text{spu}} = 0.6357 \cdot [\exp(13.5392 \cdot \varepsilon_{\text{spu}}) - 1] \quad [\text{MPa}] \qquad [17]$$

In addition, the relationship between the coefficient β and unloading strain ε_{spu}, shown in Figure 16, can also be expressed by the exponential function.

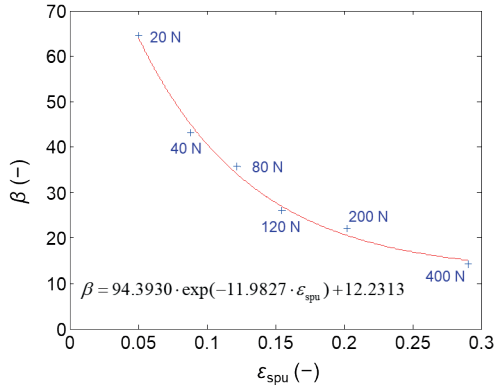

Figure 16: Relationship between the coefficients β and ε_{spu}. The discrete points are the points listed in Table 1, the red curve is the curve of the exponential function calculated by using the curve fitting method

The new function for β can be expressed as:

$$\beta = p_2 \cdot \exp(q_2 \cdot \varepsilon_{\text{spu}}) + c_2 \qquad [18]$$

where p_2, q_2 and c_2 are the coefficients for determining the unloading exponential function; the result is shown in Equation [19]. The coefficient of determination is $R^2 = 0.996$.

$$\beta = 94.3930 \cdot \exp(-11.9827 \cdot \varepsilon_{\text{spu}}) + 12.2313 \qquad [19]$$

When describing both the loading curve and the coefficient β using the exponential function, the stress–strain relation of paper can also be expressed by Equations [2] and [16] with coefficients described by Equations [12], [13], [17] and [19].

The calculation results were validated again by comparing with the experimental results.

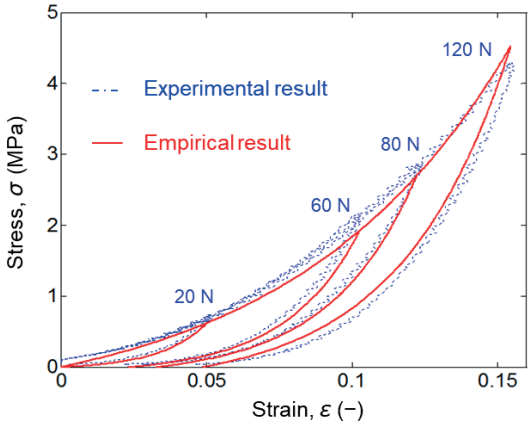

Figure 17: Comparisons between the experimental and the modified empirical stress–strain curves of paper, calculated by Equations [2], [12], [13], [16], [17] and [19]

As shown in Figure 17, the comparison results show that both of these two methods can be used for calculating the out-of-plane stress–strain relationship of paper materials; however, the fit with the former method is better (Figure 13). The calculated results based on polynomial function and exponential functions are compared in Figure 18.

It can be seen from Figure 18 that the difference between the results calculated based on the polynomial function and the exponential function is relatively small. Both of them can be used for calculating the stress–strain curve of a single sheet. Only when the stress is bigger than 4 MPa, the difference between the two curves increases.

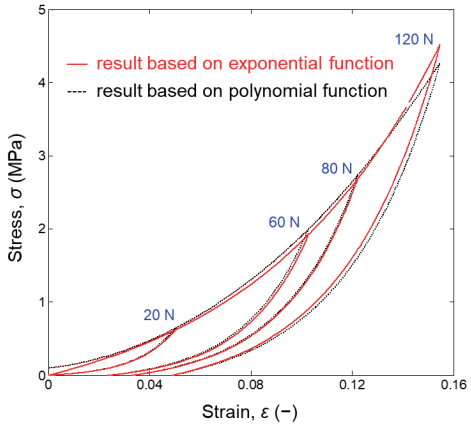

Figure 18: Comparisons of the results calculated based on polynomial function and exponential functions; the red curves are the results based on the exponential function (see Figure 17), the dashed black curves are the results based on the polynomial function, which are the red lines in Figure 13; the nominal area of the indenter is about 28.27 mm², a pressure of 3.5 MPa corresponds to about 100 N

4.2 Discussion about the force–deformation relation of multiple sheets

The described model can be used for calculating the force–deformation curve of multiple sheets. But for more sheets, the maximum number of sheets which can be calculated based on this model should be further investigated. In the following, we will discuss about the upper limit value of this model. More experiments were implemented to compare with the calculated results. The numbers of selected sheets are 72, 80, 90, 100, 110, 120, 130, 140 and 150. The comparative results between the experiment and calculation are shown in Figure 19.

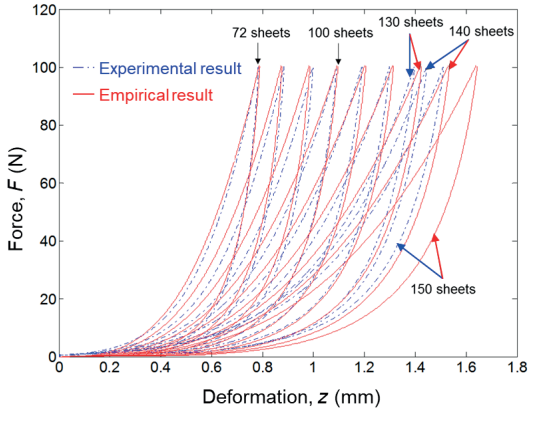

Figure 19: Comparisons of the experimental and empirical force–deformation curves of paper pile; the blue curves are the experimental data, the red curves are the force–deformation curves calculated by using the identified Equations [4] to [9] and [14] and [15]

From Figure 19 and Table 6, it can be seen that when the imposed force on the paper pile is 100 N, the maximum number of sheets which can be calculated by using this model is around 130 sheets. For further increasing the number of sheets, the deviation is increasing.

Table 6: Comparison of the force–deformation curves of paper pile between the experimental and empirical results, which is based on the deformation at the start point of unloading

Number of sheets	Deformation at the start point of unloading (mm)		Deviation (%)
	Experimental result	Empirical result	
72	0.78	0.79	−1.28
80	0.88	0.87	+1.14
90	1.00	0.98	+2.00
100	1.09	1.09	0.00
110	1.19	1.20	−0.84
120	1.30	1.31	−0.77
130	1.40	1.42	−1.43
140	1.44	1.52	−5.56
150	1.51	1.64	−8.60

In Table 6, the deviation of the deformation at the starting point of unloading has been calculated. According to Table 6, for paper piles with less than 130 sheets, the deviation between the experimental result and empirical result is smaller than 2.0 %, but when the number of sheets is 140, the deviation is increasing to about 5.6 %.

Based on the conclusion obtained above, we can redraw Figure 9 for more sheets and more forces; the new result is shown in Figure 20.

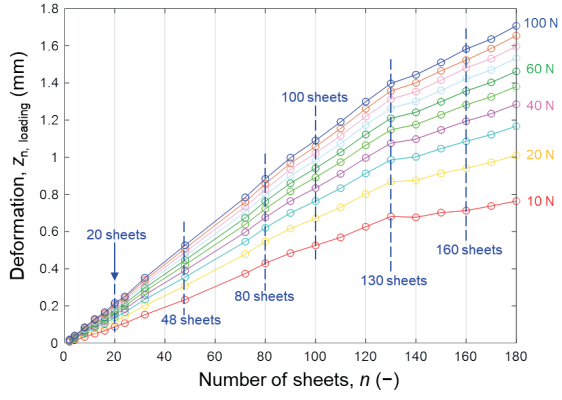

Figure 20: Experimental deformation of paper stacks under different loading forces

Figure 20 shows that when the sheet number is smaller than 130, the slopes of all curves are approximately constant values. But when the number of sheets is more than 130, the slopes will change to another con-

stant values. This figure can also prove that 130 sheets is a turning point. When compressing paper stacks, what happens when the sheet number exceeds 130, it will be another interesting research subject. But as a speculation, the authors think that with increasing the sheet number, the stress really imposed on the paper lying in the lower layer is dispersed. When the number is more than 130, the remaining part of stack (the part more than 130) probably will not be affected by the force (or pressure). The maximum force imposed here is 100 N; if the force imposed on paper stack is bigger, the maximum number of sheets that can be calculated with the proposed model will be further extended.

5. Conclusions

The mechanical behavior of paper and paper stack in the out-of-plane direction was deeply investigated in the presented study. Three main aspects of mechanical behavior of paper and paper stacks were completed, which can be summarized as follows.

Firstly, the stress–strain description model of one sheet was established and the stress–strain curves of paper under some desired strains were obtained; the comparison between the experimental result and the calculation result shows the practicability of this model.

Secondly, the stress–strain model of one sheet can perfectly be extended to calculate the force–deformation behavior of paper stacks. This aspect is based on the assumption of direct relationship between the sheet number and deformation of paper stacks at same force. The verification result under 100 N shows that the maximum number of sheets which can be calculated by this model is around 130 sheets. For other forces, the force–deformation relationship in the loading stage can be calculated by using this model, but because of the deviation of the curve fitting methods, the accuracy of the unloading calculation is not enough.

Thirdly, the model proposed for one sheet can probably be extended to some other materials (other copy paper, newsprint, paperboard, etc.) with J-shaped force–deformation curves. Some specific studies related to mechanical behavior in out-of-plane direction can be carried out according to this method. However, compared to the thickness of paperboard, paper is much thinner and the structure of paper and paperboard is also very different, which lead to some differences between the studies of paper and paperboard.

Not all models which can be used for paperboard can also be well used for thin papers, and vice versa. Therefore, the applicability of the presented model to other materials has to be verified.

Acknowledgements

The authors gratefully acknowledge the financial support from the Jiangsu Science and Technology Department (Project Number: BK20190873) as well as the Lvyang Jinfeng plan for excellent doctors of Yangzhou city. All experiments mentioned in this paper were implemented by using the testing machine ZWICK Z050 in IDD (Institute of Printing Science and Technology, Technische Universität Darmstadt).

List of Abbreviations

a_i (i = 0, ..., 6)	coefficients of the polynomial loading function
a, b, c	coefficients of the equation between β and ε_{spu}
d_{dia}	diameter of the indenter
d_{thi}	thickness of the paper
F	force
$F_{loading}$	force applied in the loading stage
$F_{unloading}$	force applied in the unloading stage
$F_{1,\ loading}$	force applied to one sheet in the loading stage
$F_{1,\ unloading}$	force applied to one sheet in the unloading stage
$F_{n,\ loading}$	force applied to n sheets in the loading stage
$F_{n,\ unloading}$	force applied to n sheets in the unloading stage
$k_{loading}$	slope in loading stage used for showing the relationship between deformation and number of paper stacks
$k_{unloading}$	slope in unloading stage used for showing the relationship between deformation and number of paper stacks
n	number of sheets
p, q	coefficients of the equation between ε_r and ε_{spu}
p_1, q_1	coefficients of the modified loading function
p_2, q_2, c_2	coefficients of the new equation between β and ε_{spu}
z	total deformation
$z_{1,\ loading}$	deformation of one sheet in the loading stage
$z_{1,\ unloading}$	deformation of one sheet in the unloading stage
$z_{n,\ loading}$	deformation of n sheets in the loading stage
$z_{n,\ unloading}$	deformation of n sheets in the unloading stage
α, β	coefficients of the exponential unloading function
σ	stress
σ_{spu}	stress at the start point of unloading
ε	strain
ε_r	residual strain
ε_{spu}	strain at the start point of unloading

References

Agilar Ribeiro, H. and Costa, C.A.V., 2007. Modelling and simulation of the nonlinear behaviour of paper: a cellular materials approach. *Chemical Engineering Science,* 62(23), pp. 6696–6708. https://doi.org/10.1016/j.ces.2007.07.053.

Alam, A., Thim, J., Manuiskiy, A., O'Nils, M., Westland, C., Lindgren, J. and Linden, J., 2011. Mechanical pulping: investigation of the surface topographical differences between the cross direction and the machine direction for newspaper and paperboard. *Nordic Pulp & Paper Research Journal*, 26(4), pp. 468–475. https://doi.org/10.3183/npprj-2011-26-04-p468-475.

Andersson, T., 2006. *A small deformation model for the elasto-plastic behaviour of paper and paperboard*. Master's thesis. Lund University.

Arango Diaz, J.M., Pfirrmann, J. and Schmitt, N., 2009. *Konzept zur blattgenauen Mengenbestimmung eines Stapels blattförmigen Materials mittels Druckstempel*. Technische Universität Darmstadt.

Borgqvist, E., Wallin, M., Ristinmaa, M. and Tryding, J., 2015. An anisotropic in-plane and out-of-plane elasto-plastic continuum model for paperboard. *Composite Structures*, 126, pp. 184–195. https://doi.org/10.1016/j.compstruct.2015.02.067.

Borgqvist, E., Wallin, M., Tryding, J., Ristinmaa, M. and Tudisco, E., 2016. Localized deformation in compression and folding of paperboard. *Packaging Technology and Science,* 29(7), pp. 397–414. https://doi.org/10.1002/pts.2218.

Chen, J., Neumann, J. and Dörsam, E., 2014. Investigation on deformation behavior of paper in Z-direction. In: *Proceedings of the Progress in Paper Physics Seminar 2014.* Raleigh, North Carolina, USA, 8–12 September 2014.

Chen, J., Neumann, J., Sauer, H.M. and Dörsam, E., 2015. A new FEM simulation method of paper materials by using a gasket model. In: P. Gane, ed. *Advances in Printing and Madia Technology: Proceedings of the 42nd International Research Conference of iarigai.* Helsinki, Finnland, 6–9 September 2015. Darmstadt, Germany: iarigai.

Chen, J., Dörsam, E., Spiehl, D., Hakimi Tehrani, A. and Da, J., 2016a. Stress–strain behavior of paper affected by the actual contact area. In: *Proceedings of the Progress in Paper Physics Seminar 2016.* Darmstadt, Germany, 23–26 August, 2016.

Chen, J., Dörsam, E., Spiehl, D., Hakimi Tehrani, A., 2016b. Elastic model of paper stacks by considering the paper structure. *Nordic Pulp and Paper Research Journal*, 31(4), pp. 648–658. https://doi.org/10.3183/NPPRJ-2016-31-04-p648-658.

DoITPoMS, 2004. Descriptions of J-shaped curves*. DoITPoMS*, [online] University od Cambridge. Available at: <http://www.doitpoms.ac.uk/tlplib/bioelasticity/j-shaped-curves.php> [Accessed May 2020].

Deutsche Institut für Normung, 2018. DIN 50014:2018-04 *Normalklimate für Vorbehandlung und/oder Prüfung – Festlegungen.* Berlin: DIN.

Eckstein, M., 2014. *Instabilities and wear propagation in calenders: interactions with structural dynamics and contact kinematics*. Doctoral thesis. Technische Universität Darmstadt.

Fukuoka, T., Takaki, T., 2003. Finite element simulation of bolt-up process of pipe flange connections with spiral wound gasket. *Journal of Pressure Vessel Technology,* 125(4), pp. 371–378. https://doi.org/10.1115/1.1613304.

Fukuoka, T., Nomura, M., Hata, Y. and Nishikawa, T., 2007. Development of test equipment for measuring compression characteristics of sheet gaskets at elevated temperature. In: *Proceedings of the ASME PVP 2007/CREEP8 Pressure Vessels and Piping Conference and The Eighth International Conference on Creep and Fatigue at Elevated Temperatures*. San Antonio, Texas, USA, 22–26 July 2007.

Fukuoka, T., Nomura, M. and Nishikawa, T., 2012. Analysis of thermal and mechanical behavior of pipe flange connections by taking account of gasket compression characteristics at elevated temperature. *Journal of Pressure Vessel Technology,* 134(2): 021202. https://doi.org/10.1115/1.4005388.

Gavelin, G., 1949. The compressibility of newsprint. *Svensk Papperstidning*, 52, pp. 413–419.

Hill, R., 1950. *The mathematical theory of plasticity*. Oxford, United Kingdom: Clarendon Press.

Huang, H. and Nygårds, M., 2010. A simplified material model for finite element analysis of paperboard creasing. *Nordic Pulp and Paper Research Journal*, 25(4), pp. 505–512. https://doi.org/10.3183/npprj-2010-25-04-p502-509.

Huang, H. and Nygårds, M., 2012. Numerical investigation of paperboard forming. *Nordic Pulp and Paper Research Journal*, 27(2), pp. 211–225. https://doi.org/10.3183/NPPRJ-2012-27-02-p211-225.

Huang, H., Hagman, A. and Nygårds, M., 2014. Quasi static analysis of creasing and folding for three paperboards. *Mechanics of Materials*, 69(1), pp. 11–34. https://doi.org/10.1016/j.mechmat.2013.09.016.

Kaulitz, T., 2009. *Bilden von Schneidlagen unter Ausnutzung des Nipinduzierten Effekts für die Druckweiterverarbeitung*. Doctoral thesis. Technische Universität Darmstadt.

Lavrykov, S., Ramarao, B.V., Lindström, S.B. and Singh, K.M., 2012. 3D network simulations of paper structure. *Nordic Pulp and Paper Research Journal,* 27(2), pp. 256–263. https://doi.org/10.3183/npprj-2012-27-02-p256-263.

Li, Y., Reese, S. and Simon, J.-W., 2017. Modelling the anisotropic deformation and delamination in laminated paperboard. In*: Proceedings of the 21st International Conference on Composite Materials, ICCM21*. Xi'an, China, 20–25 August 2017.

Litvinov, V. and Farnood, R., 2010. Modeling of the compression of coated papers in a soft rolling nip. *Journal of Materials Science*. 45(1), pp. 216–226. https://doi.org/10.1007/s10853-009-3921-x.

MATLAB Help, 2013. *Image processing toolbox: user's guide – R2013b*. [pdf] MathWorks. Available at: <http://www.mathworks.com/downloads> [Accessed May 2020].

Mäkelä, P. and Östlund, S., 2003. Orthotropic elastic-plastic material model for paper materials. *International Journal of Solids and Structures*, 40(21), pp. 5599–5620. https://doi.org/10.1016/S0020-7683(03)00318-4.

Nagata, S., Shoji, Y. and Sawa, T., 2002. A simplified modelling of gasket stress–strain curve for FEM analysis in bolted flange joint design. In: *Proceedings of the ASME 2002 Pressure Vessels and Piping Conference.* Vancouver, BC, Canada, 5–9 August 2002. ASME, pp. 53–58. https://doi.org/10.1115/PVP2002-1082.

Nygårds, M., Hallbäck, N., Just, M. and Tryding, J., 2005. A finite element model for simulations of creasing and folding of paperboard. In: *Proceedings of the 2005 ABAQUS Users' Conference.* Stockholm, Sweden, 18–20 May 2005, pp 373–387.

Pfeiffer, J.D., 1981. Measurement of the K2 factor for paper. *Tappi Journal,* 64(4), pp. 105–106.

Pino, A. and Pladellorens, J., 2009. Measure of roughness of paper using speckle. In: P.S. Huang, T. Yoshizawa and K.G. Harding, eds. *Proceedings of SPIE Vol. 7432: Optical Inspection and Metrology for Non-Optics Industries, the International Society for Optical Engineering*, San Diego, California, USA, 2–6 August 2009. SPIE. https://doi.org/10.1117/12.825072.

Ramasubramanian, M. K. and Wang, Y.Y., 1999. Constitutive models for paper and other ribbon-like nonwovens – a literature review. In: R. Perkins, ed. *Mechanics of Cellulosic Materials, AMD-vol. 231, MD-vol. 85*. New York, USA: American Society of Mechanical Engineers, pp. 31–42.

Ramasubramanian, M.K. and Wang, Y., 2007. A computational micromechanics constitutive model for the unloading behavior of paper. *International Journal of Solids and Structures,* 44(22–23), pp. 7615–7632. https://doi.org/10.1016/j.ijsolstr.2007.05.002.

Rättö, P., 2005. The influence of surface roughness on the compressive behaviour of paper. *Nordic Pulp and Paper Research Journal,* 20(3), pp. 304–307. https://doi.org/10.3183/npprj-2005-20-03-p304-307.

Schaffrath, H.-J., and Göttsching, L., 1991. The behaviour of paper under compression in z-direction. In: *Proceedings of the 1991 International Paper Physics Conference*. Kona, Hawaii, USA, 22–26 September 1991. Atlanta, USA: TAPPI Press, pp. 489–510.

Singh, S.P., 2008. A comparison of different methods of paper surface smoothness evaluation. *BioResources,* 3(2), pp. 503–516.

Stenberg, N., 2002. *On the out-of-plane mechanical behaviour of paper materials*. Doctoral thesis. Royal Institute of Technology.

Stenberg, N., 2003. A model for the through-thickness elastic-plastic behaviour of paper. *International Journal of Solids and Structures,* 40(26), pp. 7483–7498. https://doi.org/10.1016/j.ijsolstr.2003.09.003.

Takaki, T. and Fukuoka, T., 2000. Bolt-up strategy for pipe flange connections using finite element analysis. In: *Proceedings of the PVP 2000 ASME ASME Pressure Vessels and Piping Conference: Analysis of Bolted Joints*. Seattle, WA, US, 23–27 July 2000. ASME, pp. 143–150.

Takaki, T. and Fukuoka, T., 2001. Finite element analyses of bolt-up operations for pipe flange connections. In: *Proceedings of the PVP 2001 ASME Pressure Vessels and Piping Conference: Analysis of Bolted Joints.* Atlanta, GA, USA, 23–26 July 2001. ASME, pp. 141–148.

Takaki, T. and Fukuoka, T., 2002a. Systematical FE analysis of bolt assembly process of pipe flange connections. In: *Proceedings of the PVP 2002 ASME Pressure Vessels and Piping Conference: Analysis of Bolted Joints.* Vancouver, BC, Canada, 5–9 August 2002. ASME, pp. 147–152. https://doi.org/10.1115/PVP2002-1092.

Takaki, T. and Fukuoka, T., 2002b. Three-dimensional finite element analysis of pipe flange connections: the case of using compressed asbestos sheet gasket. In: *Proceedings of the ASME 2002 Pressure Vessels and Piping Conference: Analysis of Bolted Joints.* Vancouver, BC, Canada, 5–9 August 2002. ASME, pp. 171–177. https://doi.org/10.1115/PVP2002-1095.

Takaki, T. and Fukuoka, T., 2003. Methodical guideline for bolt-up operation of pipe flange connections: a case using sheet gasket and spiral wound gasket. In: *Proceedings of the ASME 2003 Pressure Vessels and Piping Conference: Analysis of Bolted Joints.* Cleveland, Ohio, USA, 20–24 July 2003. ASME, pp. 23–30. https://doi.org/10.1115/PVP2003-1869.

Teleman, A., Östlund, C., Nordström, J.-E., Johansson, P.-Å. and Vomhoff, H., 2004. *Analysis of paper surface topography under compression: STFI report CW217*. Stockholm, Sweden: STFI.

Xia, Q.S., Boyce, M.C. and Parks, D. M., 2002. A constitutive model for the anisotropic elastic-plastic deformation of paper and paperboard. *International Journal of Solids and Structures,* 39(15), pp. 4053–4071. https://doi.org/10.1016/S0020-7683(02)00238-X.